Journal of Asian Ceramic Societies 3 (2015) 92–102

HOSTED BY

Contents lists available at ScienceDirect

Journal of Asian Ceramic Societies

journal homepage: www.elsevier.com/locate/jascer

Mechanochemically synthesized high alumina cement and their implementation as low cement castables with some micro-fine additives

Vijay Kumar*, Vinay Kumar Singh, Abhinav Srivastava, P. Hemanth Kumar

Department of Ceramic Engineering, Indian Institute of Technology (BHU), Varanasi 221005, Uttar Pradesh, India

ARTICLE INFO

Article history:
Received 26 August 2014
Received in revised form
12 November 2014
Accepted 17 November 2014
Available online 4 December 2014

Keywords:
Mechanical properties
Calcium aluminate
Synthesis
Refractories

ABSTRACT

High-energy ball milling viz. mechanochemical process is being utilized to mechanically activate ceramic powders for low temperature solid state reactions. The process can help to select low-cost commercially available oxides and can produce powders with nanometer size granules. On the other hand, high alumina cement provides high service temperature when used as refractory castable. Therefore, the effects of high-energy ball milling and subsequent calcinations on the formation of high alumina cementing phases using mixtures of Al_2O_3 and $CaCO_3$ were investigated. Nano-meter sized high alumina cement (HAC) powders were synthesized by mechanochemical treatment of Al_2O_3 and $CaCO_3$ in weight ratios 7:3 and 8:2. This paper compares the calcined high alumina cement obtained by mechanically activated precursor mix for 1, 2 and 3 h. Low cement castables were prepared from calcined Chinese bauxite as aggregate matrix, prepared HAC acting as hydraulic binder and micro-fine additives as pore filling agents. The bonding of high alumina cement as well as sinterability in these castable was studied with ZrO_2, α-Al_2O_3 and SiC as micro-fine additives. Castables formulated by prepared high alumina cement demonstrate remarkably improved bulk density and apparent porosity as when compared with those prepared by commercially available cement. Casting water demand was also reduced, as a result quick setting behavior was observed. The addition of mechanochemically processed cements in refractory castables improved the thermo-mechanical properties to a significant extent.

1. Introduction

High alumina cements (HACs) or calcium aluminate cements (CACs) are the only options as a refractory cements due to their high refractoriness and are most suitable for high temperature applications [1–4]. Their hydraulic strength development is due to water bonding reactions of the calcium aluminates to form a water-resistant hydrated phases. It is a cold hydraulic bonding system. The alumina content in high performance HAC exceeds 70% Al_2O_3 and remaining is mainly CaO content. High performance concretes are possible from calcium aluminate cements and also, ultra-high strength concretes have been proposed [5–13]. The flexural strength of macro-defect-free (MDF) concrete samples based on high alumina cement show much higher values [14–16]. The difference in refractoriness between HAC and Portland cement is due to the presence of C_2S and C_3S as the main constituents of Ordinary Portland Cement (OPC), which have low eutectic points. While HAC on the other hand with high Al_2O_3 (low CaO and SiO_2) possesses a high melting point and is used as refractory cement. CA, CA_2, CA_6 and $C_{12}A_7$ are the main constituents in HAC. In addition to CA ($CaAl_2O_4$), the HAC contains major amounts of CA_2 ($CaAl_4O_7$), $C_{12}A_7$ ($Ca_{12}Al_{14}O_{33}$) phases and minor amount of un-reacted alumina. Very little amounts of C_3A ($Ca_3Al_2O_6$) is observed when samples are heated above 1500 °C. The amount of the Ca-rich phase $C_{12}A_7$ is found to decrease with time as it reacts with alumina to form CA_2 or CA whereas, the amount of CA_2 formed decreases comparatively slowly with time. HAC is used as binding materials for monolithic applications and a significant advancement in monolithic technology is the development of refractory concretes or castables [17–19]. Castables, a type of monolith, are complex refractory formulations, requiring high-quality precision-sized aggregates, modifying fillers, binders, and additives. The use of reduced cement contents in monoliths such as low cement castables and ultra-low cement castables has grown significantly over the past few years. They may be cast in molds to form specific products (pre-cast shapes) or cast “in place”, as when forming a lining for a kiln furnace.

* Corresponding author. Tel.: +91 9454749415.
E-mail address: vijaykumaritbhu@gmail.com (V. Kumar).
Peer review under responsibility of The Ceramic Society of Japan and the Korean Ceramic Society.

2187-0764
http://dx.doi.org/10.1016/j.jascer.2014.11.004

The main technical advantages of low cement castables (LCCs) and ultra-low cement castables (ULCCs) are their excellent physical properties, such as high density, low porosity, high cold/hot strengths, high abrasion and corrosion resistance. The working life of HAC in steelmaking and other ceramic industries is greatly dependent on the material's ability to withstand high temperatures without undergoing significant deformation and corrosion. Therefore, one of the approaches used throughout the later decades is to improve the performance of HAC by reduction of the liquid content formed at elevated temperatures on high-alumina refractory castables [6]. Low-melting point eutectic phases are often formed in these castables because of the reaction between Al_2O_3, SiO_2, and CaO. Outstanding gains in refractoriness have been obtained through the reduction of the amount of CaO, SiO_2 and increasing the Al_2O_3 content in the HAC. Conventionally, high alumina cements are obtained by fusing or sintering a mixture of suitable proportions of argillaceous and calcareous materials such as CaO or $CaCO_3$ and alumina (Al_2O_3) at temperatures above 1500 °C and subsequent grinding. The resultant product is a fine powder and typically has very low specific surface area (<1 m^2/g). The completion of such reactions depends on the particle size, specific surface area and the mixing of the reactant powders. Even after repeated firing grinding cycles to eliminate all of the unreacted materials, the product batch frequently contains unreacted starting materials. Recently, mechanochemical reaction has emerged as a variable method to produce nano scale materials. This technique generally influences texture and structure leading to a decrease of the particle size and simultaneously increases the micro strain due to the contribution of the grain boundaries formed during the process [20]. Mechanical activation can also be employed in order to improve the kinetics of adsorption, catalysis and mineral synthesis, as well as to customize the mineral surfaces with respect to structure and composition. Modifying the structure, composition and reactivity of the mineral surface gives rise to new applications and products [21]. It has been reported by many researchers that the mechanochemical synthesis processing can be designed in such a way as to synthesize nano-crystalline particles dispersed within a soluble salt matrix. The chemical precursors react, either during milling or in the subsequent heat treatment stage [22–29]. In the present work, a high-energy ball milling process has been applied to the mixtures of Al_2O_3 and $CaCO_3$. The reaction between Al_2O_3 and $CaCO_3$ toward cementing phase formation is obtained at much lower temperatures (~1000 °C). High energy ball milling process has a significant effect to obtain high reactivity of mixes prepared by commercial raw materials. The reaction of the oxides is initiated at temperatures as low as 900 °C. Two compositions of calcium aluminate powders containing 70 and 80 wt.% Al_2O_3 were selected. The prepared cements were characterized for their structural, mechanical and cementing properties. Finally, the calcinations temperature and time were optimized to obtain desired phases in the HAC. The effect of high-energy ball milling on the fineness of the mixtures, microstructure development of the milled powders, cementing properties and phase formation was investigated. The prime cementing phases observed, were CA, CA_2 and CA_6. Furthermore, low cement castables were prepared from calcined Chinese bauxite, prepared HAC and micro-fine additives. Here we use α-alumina, zirconia and silicon carbide as additives in castable matrix. α-Alumina is most stable and technically useful crystalline form. α-Alumina has a crystal structure based on hexagonal close packing of oxygen ions with aluminum ions occupying two out of every those octahedral voids. Inter atomic bonding though generally taken to be ionic, has significant covalent component. As a result commercial alumina is difficult to sinter and requires high temperature above 1700 °C for any significant densification. It is therefore, necessary to obtain alumina in a reactive form with submicron particle size to carryout sintering at temperature of 1550 °C. Zirconia is considered very high temperature sustaining engineering material because it shows good chemical stability, high compressive strength, good fracture strength at high temperature and low thermal expansion coefficient. This complex refractory formulation was chosen, keeping in mind the severe operating conditions of secondary steelmaking and ever demanding clean steel process requirements. Alumina-zirconia based monoliths are being used in sliding gate plates, submerged entry nozzles and ladle shrouds. Due to continuous casting operations these complex refractory shapes suffer degradation due to high abrasion. Only alumina-zirconia based materials are found to survive such operations. Carbon is sometimes added to prevent wettability from molten metal but it has very low oxidation resistance. So, submicron sized silicon carbide was used in the present work to deliver similar performance. Silicon carbide is very hard material and its addition improves thermal shock which is very much required in sub-entry nozzles. It also gets oxidized at temperatures higher than 1400 °C, therefore its addition was kept to only 1 wt.% in all castable matrixes. In the current work, X-ray diffraction results confirmed several crystalline calcium-aluminate phases. Physico-mechanical properties such as apparent porosity (AP), bulk density (BD), hot modulus of rupture (HMOR), cold modulus of rupture (CMOR) and cold crushing strength (CCS) of sintered castables were studied. The sintered castables were also characterized for their microstructure using (scanning electron microscopy) SEM.

2. Experimental procedure

2.1. Materials

The starting raw materials aluminum oxide, calcium carbonate, and zirconium dioxide were of A.R. grade and procured from Loba Chemie Pvt. Ltd., Mumbai, India. The materials were used as received. CA-25 C and CA-14 M high alumina cement used for comparative study was provided by Almatis, Kolkata, India. The Chinese bauxite, reactive alumina and silicon carbide powder were supplied by Shiva Minerals Pvt. Ltd., Rajgangpur, India. The calcined bauxite contained minimum 88.60%, 4.78%, 1.58%, 4.0%, 0.26%, 0.08% and 0.70% by weight Al_2O_3, SiO_2, Fe_2O_3, TiO_2, CaO, Na_2O and others respectively.

2.2. HAC powder preparation and phase analysis

Commercially available Al_2O_3 and $CaCO_3$ powders were used as the starting materials with 7:3 and 8:2 wt.% of Al_2O_3 and CaO. The milling operation was carried out in a QM-1SP4 type planetary ball milling system in air at room temperature for 1, 2 and 3 h. A total number of 80 stainless steel balls with a diameter of 10 mm and 2 stainless steel balls with a diameter of 20 mm were used as a milling medium in a 500 ml stainless steel vial. The milling speed was set at 600 rpm. All the samples were prepared in a glove box before the milling procedure to avoid moisture absorption. The mechanochemically prepared powders were isothermally heat treated (calcined) at the rate of 5 °C/min in air atmosphere with 1 h holding time at 1000 °C.

The phase composition and crystal structures of the prepared powders were investigated at room temperature using X-ray powder diffraction measurements. X-ray powder diffraction data were recorded at ambient conditions on a high resolution laboratory X-ray powder diffractometer at 40 kV and 40 mA. All the X-ray samples were contained in low absorbing glass capillaries of 0.3 mm diameter and sealed in a glove box under argon atmosphere using a hot wire. Data were taken from 15 to 50° at 1°/min. The samples were spun during measurement for better particle statistics. A qualitative phase analysis using the PDF-2 database (ICDD, 2003) was

Table 1
Batch composition with HAC70.

Sample	HAC70 (wt.%)	Chinese Bauxite (wt.%)	α-Al_2O_3 (wt.%)	Microfine ZrO_2 (wt.%)	Microfine SiC (wt.%)
P1	5	80	14	0	1
P2	5	80	12	2	1
P3	5	80	10	4	1
P4	5	80	8	6	1
P5	5	80	6	8	1
P6	5	80	4	10	1
P7	5	80	2	12	1
P8	5	80	0	14	1

Table 2
Batch composition with HAC80.

Sample	HAC80 (wt.%)	Chinese Bauxite (wt.%)	α-Al_2O_3 (wt.%)	Microfine ZrO_2 (wt.%)	Microfine SiC (wt.%)
Q1	5	80	14	0	1
Q2	5	80	12	2	1
Q3	5	80	10	4	1
Q4	5	80	8	6	1
Q5	5	80	6	8	1
Q6	5	80	4	10	1
Q7	5	80	2	12	1
Q8	5	80	0	14	1

used to identify the phases. Crystallite size, d of calcined powder was calculated from X-ray line broadening analysis using Scherer's formula:

$$d = \frac{0.9\lambda}{\beta \cos\theta}$$

where β is the full width at half maximum (FWHM) intensity of a Bragg reflection excluding instrumental broadening, λ is the wavelength of the X-ray radiation and θ is the Bragg angle. β is taken for strongest Bragg's peak corresponding to 2θ.

Bright field transmission electron microscope (FEI, Eindhoven, Netherlands) equipped with SIS Mega View III CCD camera at 120 kV employing Analysis software (SIS, Muenster, Germany) was used for TEM investigations. Powder samples for TEM were first dispersed in suitable solvent by ultra-sonication and then dropped on a conventional carbon coated copper grid.

2.3. Consistency and setting time of cement prepared

(a) Consistency is a measure of the plasticity of a cement paste. It refers to the degree of wetness exhibited by a freshly mixed concrete, mortar or neat cement ground whose workability is taken into account acceptable for the aim at hand. It is measured as the amount of water needed on a specific wt.% of dry cement which allows the Vicat's plunger of 10 mm diameter to penetrate to some extent 5–7 mm from the lowest of Vicat's mold with gauging time 3–5 min. Calcined HAC powder having 70 and 80 wt.% alumina content samples were tested for consistency by Vicat's equipment.

(b) Initial setting time: The early period in the hydration and strengthening of cement is referred as "initial setting" of cement. The initial setting time was measured by taking 50 g of HAC mixed with the percentage of water required for the normal consistency. In Vicat's apparatus a needle is allowed to penetrate through the cement block prepared. In the initial stage, a thicker needle is allowed to pierce through the test block. This procedure is repeated until the paste starts losing its plasticity, and the penetration is limited only to 5–7 mm depth. This duration of setting was counted and termed as the initial setting time.

(c) Final setting time: The cement will be considered final set when, upon, falling the final setting plunger gently covers the surface of the test block and the needle makes no impression. The duration up to this process is considered as the final setting time (ASTM C403).

2.4. Castable formulation

Low cement refractory castables were prepared using 5 wt.% prepared HAC cements, 7 wt.% water and refractory bauxite. Small additions of zirconia, reactive alumina and micro-fine silicon carbide powder particles were done as pore filling agents. The effects of different additives on the development of castable refractories have been studied by a number of researchers. ZrO_2, reactive alumina and micro-fine SiC have also been reported to improve the thermal shock, CCS, CMOR and HMOR, as well as the densification of bauxite based castables. The formulation presented in Tables 1 and 2 shows the detailed composition with their names. Bauxite particle size distribution is shown in Fig. 1. In the first step for cement castable formulation, calcined bauxite was oven dried, crushed, and

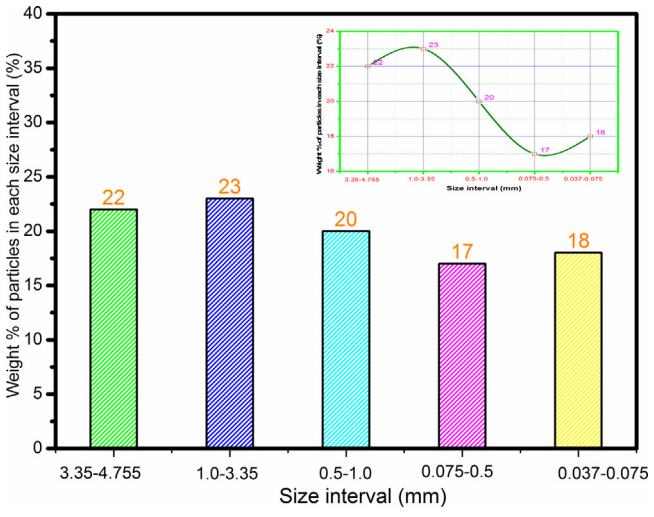

Fig. 1. Particle size distribution of castable matrix.

ground in a planetary ball mill, for grading into different sizes. The particle size distribution has an important role in the properties of refractory castable. Incorrect particle size distribution may cause militancy or the excess water required by the castables. The particle size distribution of the fine fraction is generally a representation of the flow characteristics. The use of particle packing principles provides the basis of the development of castable with low porosity, means for achieving high compaction in castable. The fine materials replace the part of cement of conventional castables. These micro-fine materials play three major roles; first to fill up the voids between cement particles which reduce the water requirement for achieving the same consistency and also reduces the porosity, increasing density. Secondly, these fine particles have shown some effect on fluidity. Thirdly, the nature of fine particles has shown some effect on the phase composition of the matrix at elevated temperature. Thus the nature of ultra-fine particles decide the high temperature properties like creep behavior, corrosion resistance and hot strength. The trials of aggregate proportions were taken in a 1000 cm^3 flask filled up to 250 cm^3 and vibrated for 45 s and the packing density calculations were carried out for each trial. Aggregates having higher packing densities were chosen for further experiments. In the next step, batches were prepared by taking different grades of materials and additives in the proper proportion and which are summarized in Tables 1 and 2. The materials were dry mixed in a plastic container for 20 min and then were taken for sample preparation. The casting was done by adding the first two-thirds proportion of water at a time. Then, remaining of water was added slowly to get a homogeneous mixing. The wet mixing was performed for up to 8–10 min to achieve proper flow. Immediately after wet mixing, the castable mix was filled into a rectangular bar shape mold (152 mm × 25 mm × 25 mm) made of hard steel. The mold was placed on the vibrating table filled with the wet mixed castable. It was vibrated for 20 min resulting in better compactness. Several samples of each composition were prepared for laboratory test. The samples were cured in a humidity chamber (95% RH) at room temperature for different time periods. Before firing the samples, they were first oven dried at 120 °C for 24 h. The test samples were fired at 1300–1550 °C with a variation of ±5 °C in an electric SiC heating element furnace with a soaking time of 3 h. The cured samples as well as the fired samples were tested for BD, AP, TSR, HMOR, CMOR and CCS. These samples were also analyzed by XRD for crystalline phases present and by SEM for their morphological behavior. The commercialized cement castables were also prepared for comparison purposes.

2.5. Cold crushing strength of HAC and LCC formulated

It is the ability of a material to resist axially directed pushing forces. By definition, the compressive strength of a material is that worth of uniaxial compressive strength reached when the material fails fully. CCS of cement was measured as the compressive strength of a 50 mm cement cube made of pure HAC. These samples were tested for compressive strength after 6 h, 24 h and 7 days according to ASTM C1194-03. Similarly castable prepared in cube shapes, fired at varying temperatures were employed for this measurement.

2.6. Cold and hot modulus of rupture (CMOR and HMOR) of LCC formulated

Cold and hot modulus of rupture measurements were carried out under three-point bending tests (ASTM C133-97 for CMOR and ASTM C583-10 for HMOR) using dimension 152 mm × 25 mm × 25 mm of samples. CMOR and HMOR were calculated using the following formulae:

$$\text{MOR} = \frac{2PL}{2db^2}$$

CMOR tests were carried out at room temperature using a UTM machine (Model 810, MTS System, Eden Prairie, MN, USA) of samples pre-fired at 1300, 1350, 1400, 1450, 1500 and 1550 °C for 3 h. HMOR measurements were made at 1400, 1500 and 1600 °C using the Netzsch 414/3 HMOR Equipment (Netzsch Selb, Germany) of samples pre-fired at 1550 °C for 3 h, cooled to room temperature and then reheated for testing.

2.7. A.P., B.D., TSR and SEM of prepared castables

Apparent porosity and bulk density were determined according to ASTM C20-00 which involves boiling water bath principle. Cyclic thermal stability of the refractories was determined experimentally by water quench test; ASTM C1171-05. The thermal shock resistance (TSR) is measured by the number of cycles a specimen survives without any visible damage appearance, when the specimens are subjected to thermal cycling. This effect was evaluated after each cycle of consecutive firings at 1000 °C and then subsequent water quenching at 25 °C for 20 min. This firing was done in an electric furnace containing SiC heating elements. The microstructural evolution of castables fired at 1550 °C was examined using field emission scanning electron microscopy of representative regions of fractured specimens. All samples were prepared after initial grinding, further grinding was done in two steps, i.e. with 240, 320, 400 and finally 600 grit SiC abrasive paper. The samples were then polished on velvet cloth impregnated with 6 μm and finally with 1 μm diamond paste. Water was used as a lubricant. After final polishing samples were etched with mixture of HCl and HNO_3 samples were then coated with carbon unit to make it conductive. Silver paste was used on the corners of the samples to avoid any charging during testing.

3. Results and discussion

3.1. Evolution of phases by X-ray diffraction

Fig. 2 shows the XRD patterns of a mixture of Al_2O_3 and $CaCO_3$ milled for different time durations. For the samples milled for 1–3 h the diffraction peaks visible are attributed to $CaCO_3$. These

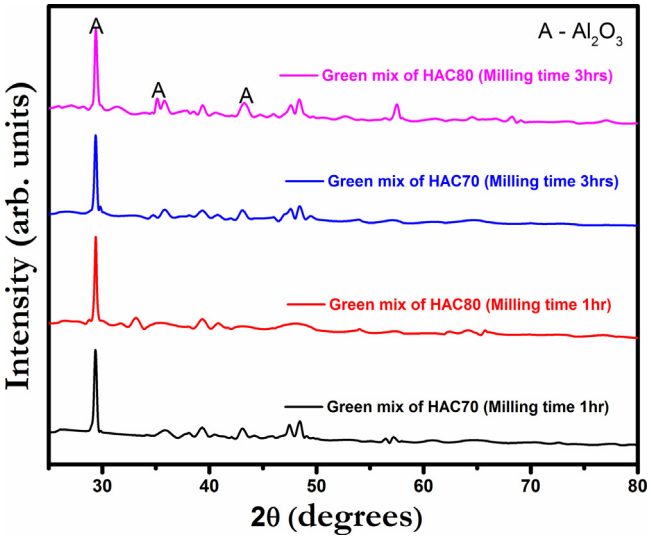

Fig. 2. XRD plot of pure milled HAC powder.

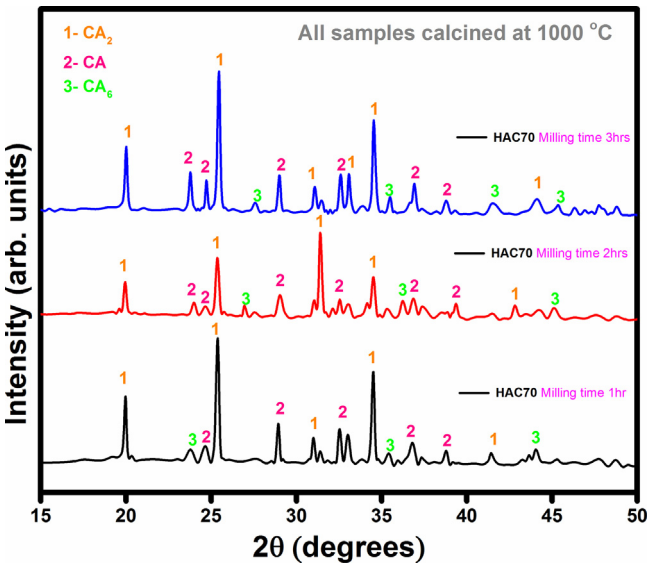

Fig. 3. XRD plot of HAC70.

significant peaks even after 3 h of intense milling in the planetary mill can be taken as a further indication of the high milling resistance and mechanical strength of their nano particles. No Al_2O_3 peak is evident as it exists in amorphous phase. $CaAl_2O_4$ diffraction peak is also not observed indicating no phase formation at this stage. Nano-meter range powder is formed as a result of high energy ball milling when attrition time increases to 3 h. Figs. 3 and 4 demonstrate the XRD patterns of samples calcined at 1000 °C with 70 and 80 wt.% alumina termed as HAC70 and HAC80 respectively. Pure crystalline cementing phases only begin to form when the temperature is 1000 °C in both HAC70 and HAC80 compositions. A major improvement in crystalline behavior is evident when both cement samples were fired at 1000 °C. Prime phases investigated in both compositions include CA, CA_2 and CA_6, which are readily formed and thermodynamically most stable compounds in the $CaO–Al_2O_3$ binary system. These peaks were identified by standard JCPDS cards numbered 88-2477, 89-3851 and 07-0085 for their corresponding peaks of monoclinic CA, CA_2 and hexagonal CA_6 respectively. In the conventional preparation route by high-temperature solid-state synthesis,

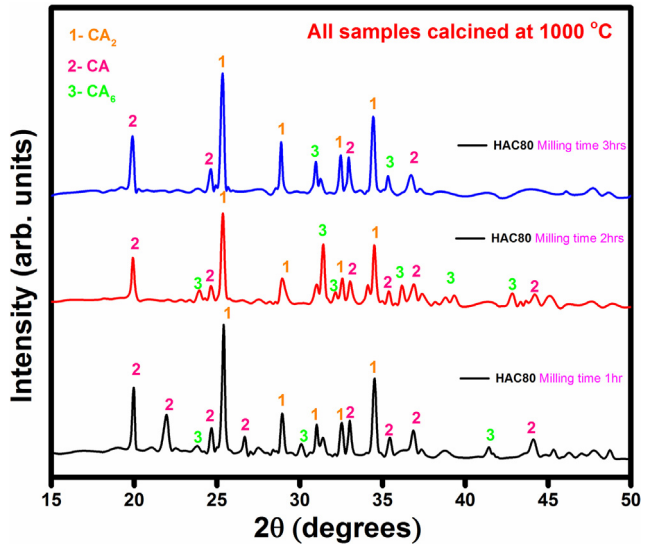

Fig. 4. XRD plot of HAC80.

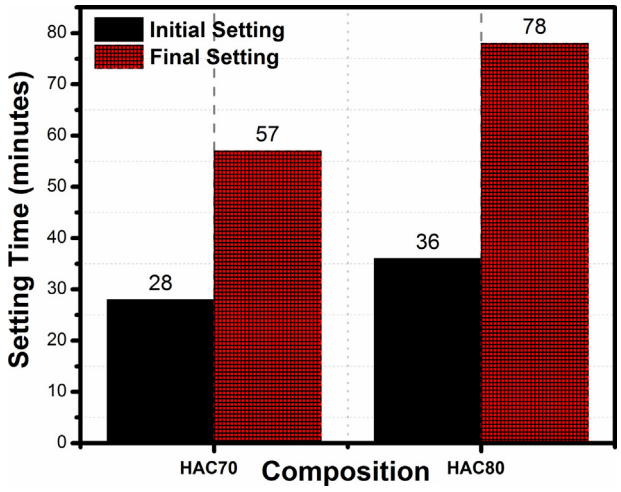

Fig. 5. Setting time behavior of HAC70 and HAC80.

the batch usually contains CaO-rich phases and unreacted Al_2O_3 before the appearance of desired product phase. The formation sequence of phases in these mixtures is always from calcia-rich phases to the alumina rich phase. Presence of broad peaks in XRD patterns of calcined cement powders shows that particle size is small.

3.2. Cementing behavior of HAC

Fig. 5 shows the setting behavior of HAC. The prepared HAC powders were mixed with water (0.85 P). At room temperature (26 °C), 70 wt.% alumina containing cement gave an initial setting time of 28 min and final setting occurred in 57 min. Second composition of HAC having 80 wt.% alumina had an initial setting time of 36 min and a final setting time of 78 min. In initial curing stage, the strength is obtained by coagulation of the polyvalent ion from the alumina cement. This initial set provides sufficient strength for the core (frame mold) removal. It is observed that with increasing alumina content the setting time exhibited an increasing trend. High alumina content results in increased formation of CA_6, which does not takes part in hydration reaction but is necessary for high temperature strengths. Presence of this phase increased setting time of the prepared cement as when compared with standard commercial products and thus an improvement in workability of cement pastes was observed.

3.3. CCS of HAC fired at 1000 °C

The pure high alumina cement attained good structural strength as obtained from experiments presented in Fig. 6. Samples were tested after curing for 6 h, 24 h and 7 days. Sample blocks of two commercialized cements of similar compositions were also prepared to have a better comparative result. The strength increased rapidly with curing time in all the compositions. Initially, in 6 h, the CCS value obtained for HAC70 is 12 MPa and for HAC80 is 15 MPa. After 7 days it reached up to 89 and 96 MPa for HAC70 and HAC80, respectively, which is better than the commercially available CA-14M (76 MPa) and CA-25C (84 MPa). It gets the maximum strength at around 7 days and after this period there is a very slight variation. It can be seen that HAC80 samples have more compressive strength than the HAC70 sample. The higher strength of HAC80 is ascribed to the presence of larger amounts of CA_6. It is a well-known fact that mono-calcium hexaluminate (CA_6) phase is very stable and high temperature sustaining phase. The most significant advantage of this phase is its needle and platelet like

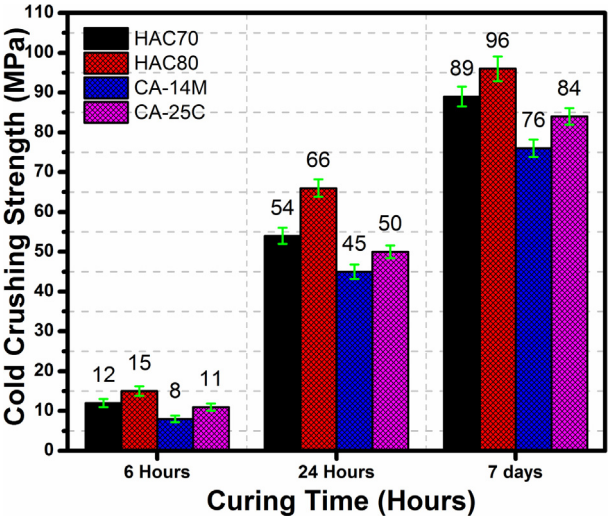

Fig. 6. Cold crushing strength of HAC70 and HAC80.

morphology growth, which is rarely formed through novel low temperature diffusion mechanism. Improved mechanical properties result from in situ whiskers or platelets formation. Dispersion of shaped CA_6 within the matrix enhanced crushing strength by crack defection and grain bridging mechanisms. These mechanisms dissipate considerable strain energy through frictional motion of the reinforcement phase against the matrix during elastic stretching, debonding and pullout [30]. Thus, an increase in the number, diameter, and debond length of such bridging reinforcements is expected for the enhanced toughening effects [31]. Although CA_2 is known to react slowly with water in the early stages of hydration, its presence along with other phases results in an overall faster hydration rate as the heat of hydration resulting from the hydration of CA activates CA_2 and makes it react relatively faster with water than it would do alone. Present outcomes are efficacious and analogous with mineralogical studies by XRD, exhibiting high structural strength in both the samples. This is due to the formation of the stable ceramic bond and the absence of any impure phase.

3.4. SEM and TEM of prepared HAC

Fig. 7(a) and (b) represents the SEM of networks of well-crystallized interlocking hexagonal plates of CA matrix of HAC70 and HAC80 fired at 1000 °C, respectively. In both figures 1–4 represents different magnifications (1000×, 5000×, 10,000× and 20,000×) of the same samples. The monoclinic phases of CA, CA_2 and hexagonal phase of CA_6 can be observed in both micrographs. High amounts of CA and CA_2 are proposed to enhance

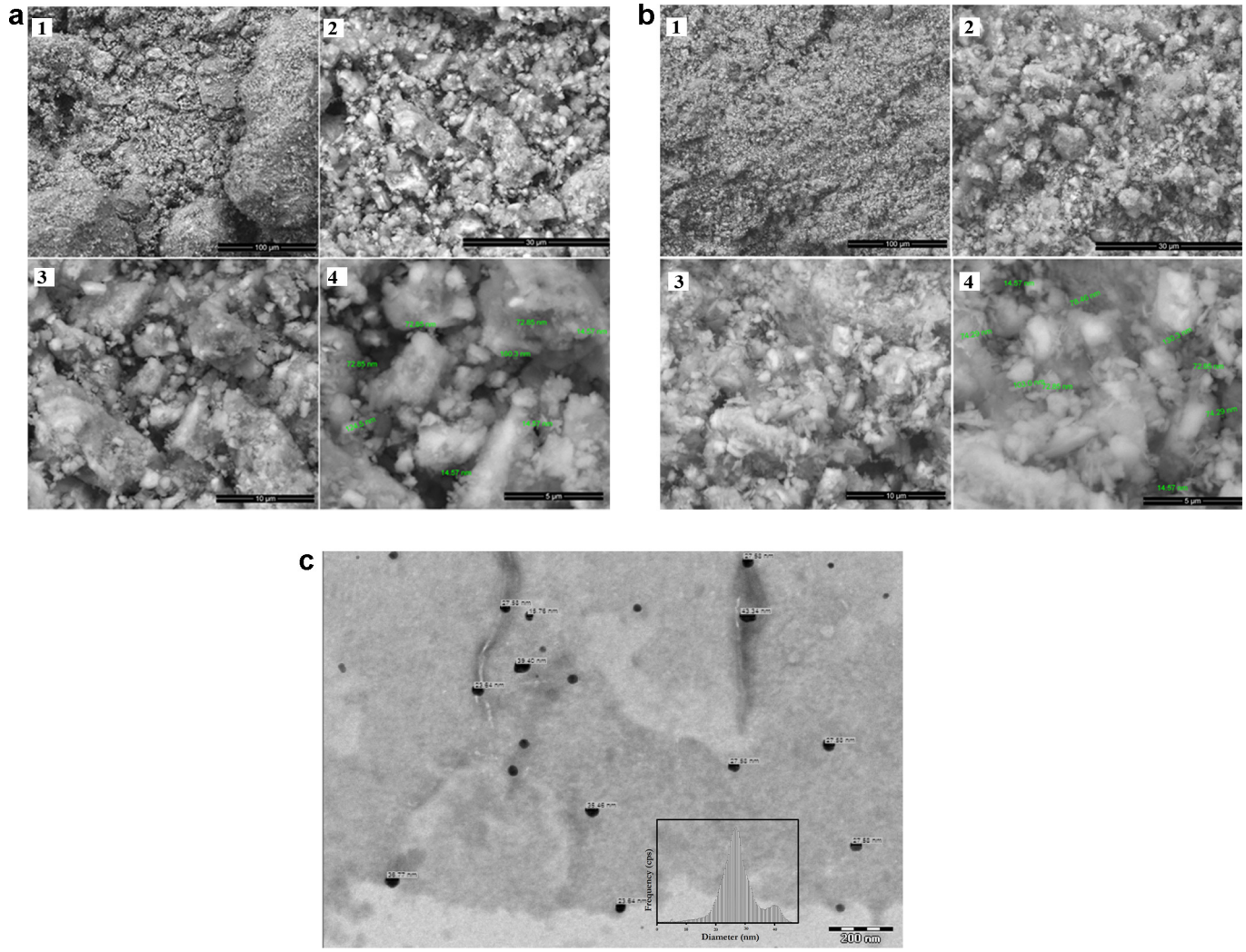

Fig. 7. SEM of (a) HAC70 and (b) HAC80. (c) TEM of HAC80.

Table 3
Bulk density, apparent porosity and thermal shock cycles of prepared castables.

Test method	Temperature (°C)						
	Sample name	1300	1350	1400	1450	1500	1550
Bulk density (g/cm^3)	P6	2.90	2.95	3.00	3.25	3.28	3.31
	P6 (CA-14M)	2.85	2.91	2.96	3.21	3.15	3.20
	Q6	3.05	3.15	3.26	3.35	3.39	3.42
	Q6 (CA-25C)	2.94	3.05	3.16	3.26	3.30	3.32
Apparent porosity (%)	P6	9.6	9.5	8.8	8.6	8.2	8.0
	P6 (CA-14M)	11	10.6	9.8	9.4	9.2	9.1
	Q6	7.9	7.8	7.6	7.5	7.1	6.6
	Q6 (CA-25C)	9.2	8.8	8.5	8.2	8.1	7.8
Thermal shock cycle	P6	18	15	15	14	15	19
	P6 (CA-14M)	17	16	14	12	14	18
	Q6	19	17	16	15	16	22
	Q6 (CA-25C)	16	15	17	12	14	18

Table 4
Relative crystallinity of major crystalline phases obtained from XRD patterns best compositions.

Sample	Relative crystallinity (%)				
	α-Al_2O_3	$3Al_2O_3{\cdot}2SiO_2$	ZrO_2	SiC	Unidentified peaks
P6	69.7	16.5	9.6	0.7	3.5
Q6	70.5	17.6	9.8	0.8	1.3

the refractory properties. The morphology of CA_6 grains shows preferential growth along their basal plane. After CA_6 formation, the main mechanism responsible for grain growth is the welding of neighboring platelet grains when they are disposed with their flat boundaries, and thus with their basal planes, parallel. For this reason, platelet grains become more equiaxed as firing temperature increases. When grains are equiaxed, the proportion of grains with basal planes parallel is very low, so the increase in firing temperature does not much affect grain granulometry. Fig. 7(a) and (b) illustrates the presence of both mechanisms: grain impingement and plate welding. CA_6 phase is responsible for high strength at high temperature without rapid physical and chemical deterioration. Major parts of trigonal crystals in cementing phase are evident in the most homogeneous distribution of CA and CA_2 phase matrix.

Fig. 7(c) shows the particle size and crystallinity of the prepared HAC80 powder produced by mechanochemical synthesis which was investigated by TEM. Numerous crystals were isolated in dispersed form, mostly in perfect spherical shape. Their growth along their circumference indicates that reaction propagated equally from all directions providing sufficient room for overall circumferential growth. HAC80 produced the loosely agglomerated, fine particles of an average 40 nm diameter.

3.5. XRD patterns of castables fired at 1550 °C for 3 h

X-ray diffraction of sintered samples of high alumina cement based castable compositions was done to estimate the phases present after sintering at 1550 °C temperature. Extent of reaction was estimated from the amount of the different phases present. Table 4 shows the evaluation percentage of relative crystallinity. Description of this estimation is given elsewhere [32–35]. X-ray diffraction was done for all samples, sintered at 1550 °C with same soaking period to study the extent of reaction and to correlate the reaction behavior with phase formation. Figs. 8 and 9

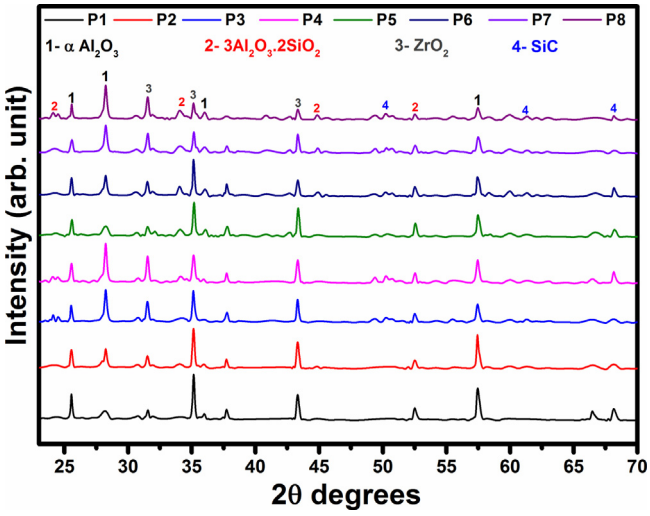

Fig. 8. XRD plot of P series castables prepared with HAC70.

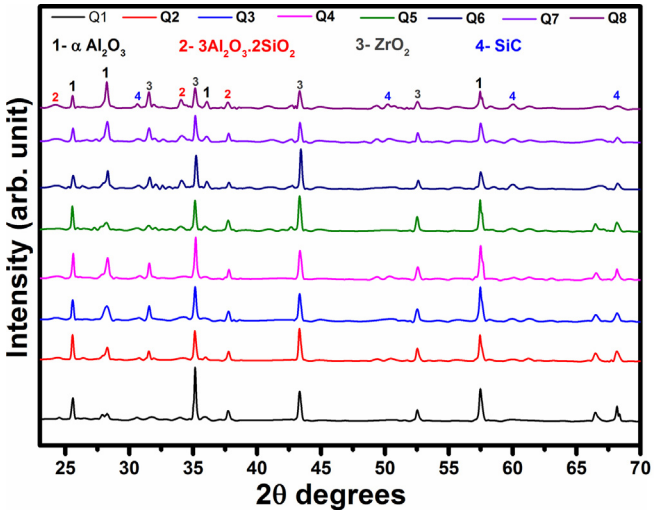

Fig. 9. XRD plot of Q series castables prepared with HAC80.

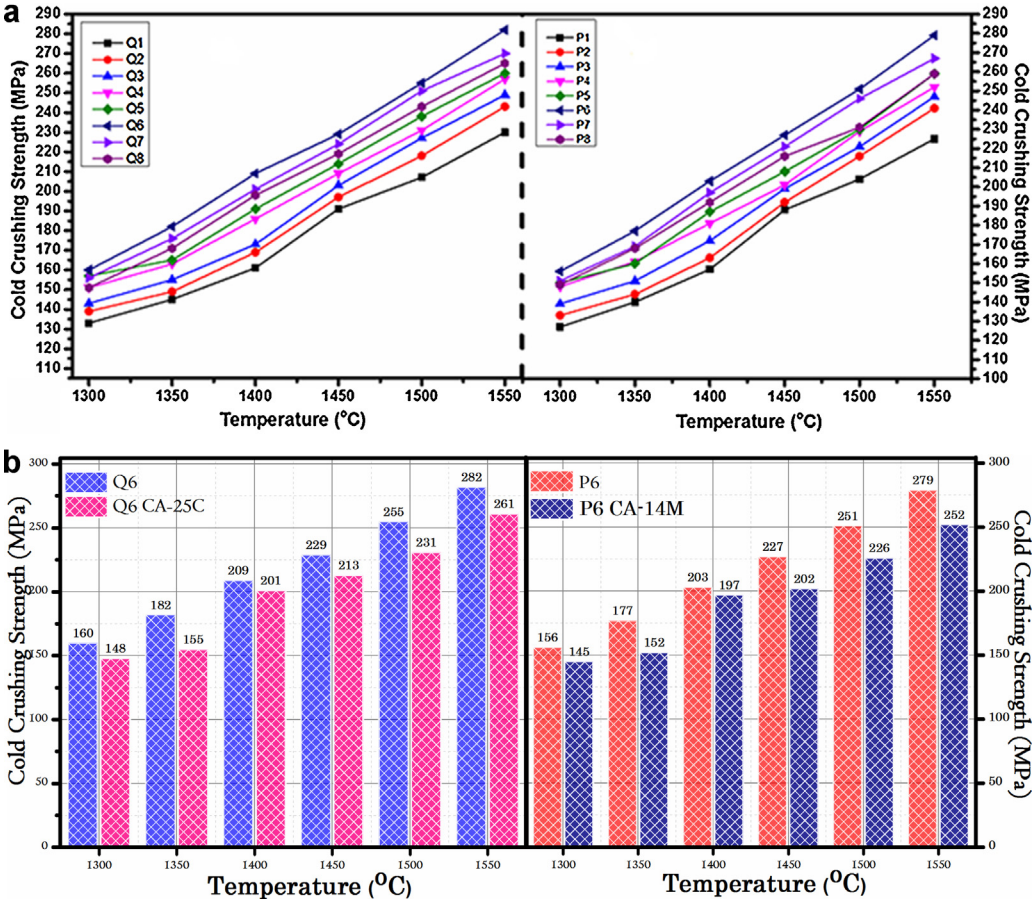

Fig. 10. (a) Cold crushing strength of castables. (b) Compared cold crushing strength of castables.

portray XRD patterns of castables fired at 1550 °C for 3 h, here P (1–8) and Q (1–8) indicate a series of castables formulated with HAC70 and HAC80, respectively. The corundum phase appeared as a major component due to the transformation of bauxite minerals to corundum. Other major phases detected were zirconia and mullite. Silicon carbide also occurred as a minor peak, which was in correlation with the slight addition of silicon carbide in all the castable samples. In both castable series P and Q, as we proceed from high to low batch number, the peak intensities increase, this is accounted for increasing micro fines. These peaks were identified by standard JCPDS cards numbered 46-1212 (Al_2O_3), 15-0776 ($3Al_2O_3{\cdot}2SiO_2$), 42-1091 (SiC) and 78-1807 (ZrO_2).

3.6. Bulk density, apparent porosity and thermal shock cycles of prepared castables

Table 3 displays the values corresponding to bulk density, apparent porosity, and thermal shock of P6 and Q6 series castables sintered at varying temperature range. Only these series was selected as homologous to their other thermo-mechanical superiority. In the castables prepared, highest bulk densities achieved are 3.31 and 3.42 g/cm^3 for the compositions P6 and Q6, respectively as when compared with 3.21 and 3.32 of their commercial cement based castable counterparts. This can be attributed to the use of higher percentages of micro-fine ZrO_2, α-Al_2O_3 and SiC in the aggregate as well as CA_6 formation. Apparent porosity was measured to be in the range of 6.6–9.6% in the castables prepared though it was 9.1 and 7.8 for P6 (CA-14M) and Q6 (CA-25C) respectively. Table 3 shows the number of thermal shock cycle values evaluated for P6 and Q6 series castables. This series was chosen in agreement with their superior mechanical properties. All the Q and P series samples exhibited high spalling resistance completing 10 cycles while P6 and Q6 attained 19 and 22 cycles respectively. Commercial cement containing castables also achieved 18 cycles.

3.7. CCS of different castable compositions sintered at 1300–1550 °C for 3 h

Prepared high alumina cement was used for formulating low cement castables according to Tables 1 and 2. Micro-fine ZrO_2, α-Al_2O_3 and SiC content has been varied, which according to the above mentioned plots resulted in corundum and mullite phase formation along with existing phases. This formation of phases also has a varying effect in the CCS of the castables formulated. Fig. 10(a) depicts the castable series Q and P. High values of CCS ranging 160–282 MPa was achieved at the maximum sintering temperature 1550 °C for Q series castables. Similarly, 156–279 MPa was achieved for P series castables. Fig. 10(b) represents a comparative crushing strength plot of Q6 series castables prepared with synthesized and commercial cement. It can be predicted that the rise in sintering temperature has a positive effect on the mechanical properties of both series of castables. Formation of corundum as well as the addition of zirconia strengthens the structure at high temperatures and some mullite solid solution helps in increasing structural strength; silicon carbide also plays very important role in improving the CCS value of all the castable [36–39]. The CCS of the castables prepared with HAC70 and HAC80 were higher in comparison with the CCS of conventional bauxite containing LCC prepared with CA-14M (136 MPa) and CA-25C (220 MPa).

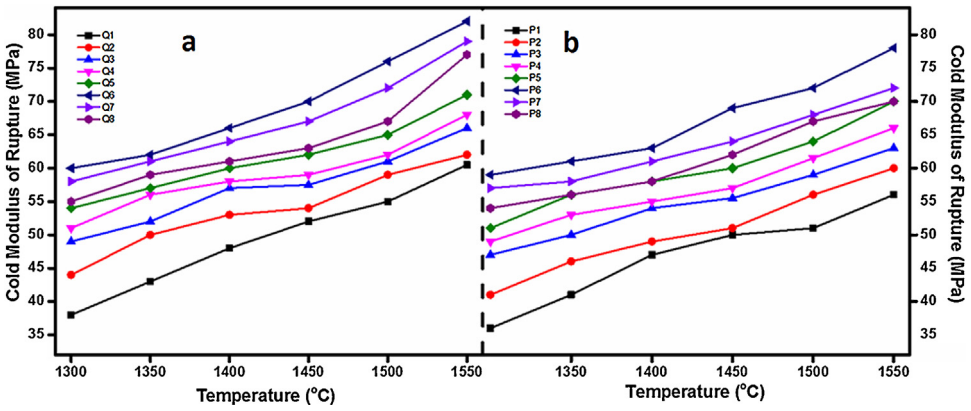

Fig. 11. Cold modulus of rupture of castables. (a) Q series and (b) P series.

3.8. CMOR and HMOR of prepared castable

Cold modulus of rupture of castables Q and P series is displayed in Fig. 11(a) and (b). It can be observed that values as high as 82 MPa can be obtained, even if apparent porosities are near 9%. The flexural strength of a ceramic material is linked to both its density and pores morphology. Usually, an increase in firing temperature leads to an increase in density and accordingly in flexural strength. This behavior is followed by both series castables and it is found to be highest for Q6 in which maximum amount of corundum, mullite, zirconia and silicon carbide phase was identified. Hot modulus of rupture (HMOR) of castables Q and P series is shown in Fig. 12(a) and (b), respectively. Here, again Q6 achieved the maximum strength at high temperature/load. The increase in HMOR values of few samples from 1400 to 1600 °C is due to the increased formation of corundum and mullite solid solutions. To clinch we may say that the safe range for these types of castables at higher loads is lower than 1600 °C. The impurities in the bauxite aggregate increase the liquid phase sintering and decrease the porosity which consequently increases the mechanical properties.

3.9. SEM of Q1–Q8 castable

Fig. 13(A)–(H) depicts SEM photomicrographs of Q series castables after firing at 1550 °C for 3 h (at 10,000× magnifications). Only Q series castables were chosen for analysis through SEM as they represented superior thermo-mechanical and physical properties than P series castables. All micro-plots indicate that the examined samples have a dense crystalline structure with a high rate of grain growth of corundum, mullite and zirconia as well as the direct bonding of the same crystals. The presence of abundant corundum trigonal phase is noticed in all microstructures. The high alumina cements bonding phases which were traced in all 8 compositions, occur in low amounts, mainly at the grain boundaries of corundum, mullite and zirconia, so they practically do not reduce the refractoriness of the materials. In Fig. 13(A) and (E) the matrix includes CA and some liquid phases. SEM photomicrographs in Fig. 13(B) and (C) exhibit densely packed microstructure of micronized zirconia, embedded in the trigonal corundum matrix. As we proceed to micrograph Fig. 13(F)–(H), some acicular mullite beside corundum grains appeared in the microstructure. The presence of such in situ formed phase (mullite) provided interlocking of grains and reinforced the matrix confirming the high strength and refractory properties of castables. The impurities such as silica that was present in Chinese bauxite could be accounted for a mullite solid solution formation, which tend to increase the refractory properties. The influence of trace impurities presented during the processing of ceramics is well known and exploited in the control of densification, grain growth and morphology during sintering. The ability to control microstructure is important for achieving the desired properties.

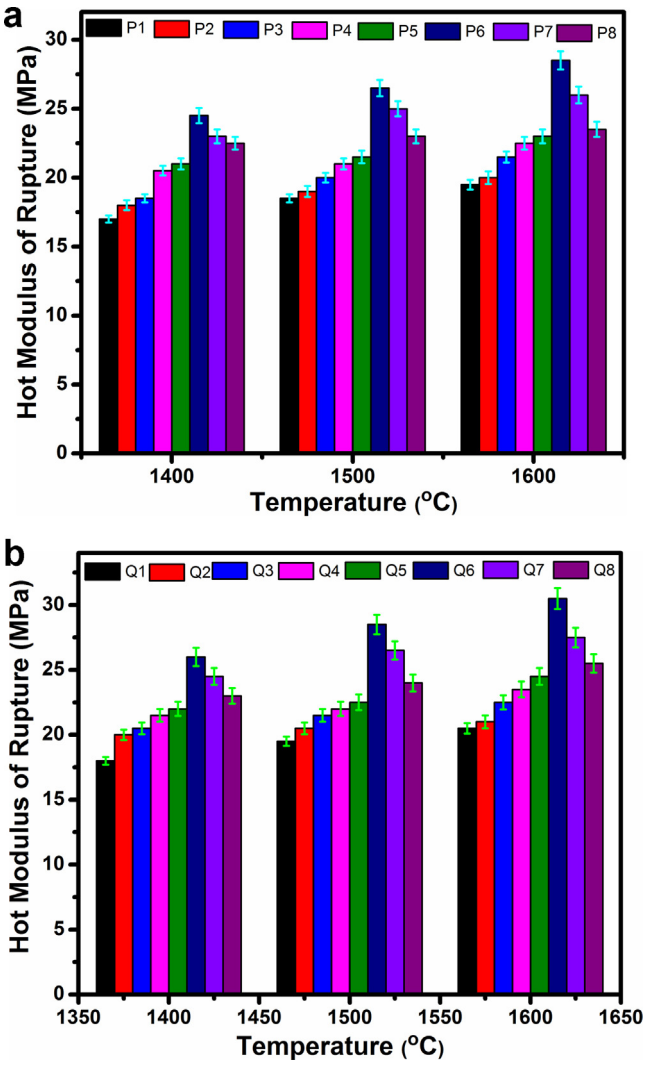

Fig. 12. Hot modulus of rupture of castables prepared with (a) HAC70 and (b) HAC80.

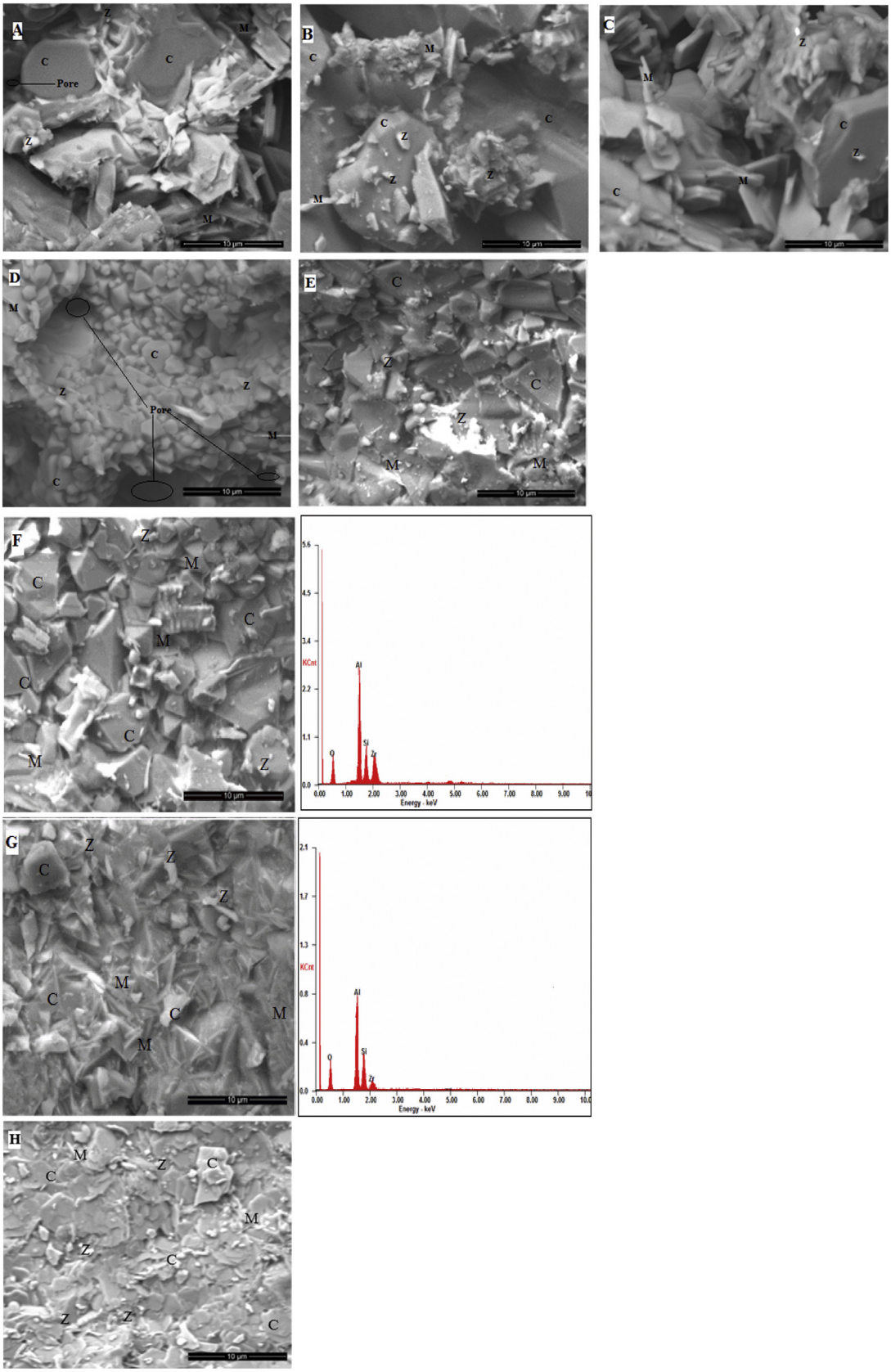

Fig. 13. SEM of (A) Q1, (B) Q2, (C) Q3, (D) Q4, (E) Q5, (F) Q6, (G) Q7 and (H) Q8 castable prepared with HAC80.

4. Conclusion

In the first portion of the study, high alumina cement was mechanochemically synthesized at 1000 °C. HAC thus prepared had very small crystallite size. Cementing behavior promises a new era of industrial evolution through commercial implementation. Desired cementing phases CA, CA_2, and CA_6 were formed at a very low temperature. One advantage of this process is to exclude silicate phases which are the cause behind eutectic formations in such cements. These silicate phases if any, decrease the refractoriness and the cement is not suitable for high temperatures.

The second part of the study is focused on the influence of this prepared cement on formulated castables. The XRD patterns of castables containing bauxite, micro-fine ZrO_2, α-Al_2O_3 and SiC evolved new and pure phases such as corundum, mullite along with pre-existing zirconia and SiC. The formation of CA_6 and absence of silicate phases in cement were responsible for superior thermo-mechanical and physical properties as when compared with commercial cement containing castables. Castable samples prepared by HAC80 have better mechanical properties than the HAC70 even though it had lower setting time. Trigonal corundum and acicular mullite formed at high temperature facilitate ceramic bonding which were termed responsible for an increase in the CCS and CMOR. Pea sized grains of corundum improved thermal cycles. SEM represents dense microstructure of all the samples. Some liquid phase is also visualized due to the impurities present in bauxite. These excellent properties of such castables enable their use in various refractory applications such as fabrication of steel, aluminum, copper, glass, cement, chemicals, and ceramics.

References

[1] A.R. Studart, R.G. Pileggi and V.C. Pandolfelli, Am. Ceram. Soc. Bull., 80, 34–40 (2001).
[2] A.R. Studart and V.C. Pandolfelli, Am. Ceram. Soc. Bull., 79, 53–60 (2000).
[3] N.M. Khalil, S.A.S. El-Hemaly and L.G. Girgis, Ceram. Int., 27, 865–873 (2001).
[4] J. Mori, W. Watanabe, M. Yoshimura, Y. Oguchi and T. Kawakami, Am. Ceram. Soc. Bull., 69, 1172–1176 (1990).
[5] M.T. Gaztanaga, S. Goni and J.L. Sagrera, Solid State Ionics, 63, 796–802 (1993).
[6] S. Kumar, S.K. Das and P.K. Daspoddar, Ceram. Int., 29, 139–144 (2009).
[7] S.A. Abo-El-Enein, M.M. Abou-Sekkina, N.M. Khalil and O.A. Shalma, Ceram. Int., 36, 1711–1717 (2010).
[8] K. Mori, Y. Toritani and S. Tanaka, in Fourth Biennial Worldwide Conference on Refractories: Global Development of Refractories, Ed. by T.G. Kyōka, UNITECR, Kyoto, Japan, November (1995) pp. 171–178.
[9] K. Furuta, K. Ido and Y. Kawase, Taikabutsu, 47, 501–502 (1995).
[10] B. Stenly and S.B. Lansday, Ind. Heating, 64, 55–57 (1997).
[11] D. Asmi and I.M. Low, Ceram. Int., 34, 311–316 (2008).
[12] E.Y. Sako, M.a.L. Braulio, D.H. Milanez, P.O. Brant and V.C. Pandolfelli, J. Mater. Process. Technol., 209, 5552–5557 (2009).
[13] E.Y. Sako, M.a.L. Braulio and V.C. Pandolfelli, Ceram. Int., 38, 2177–2185 (2012).
[14] J. Li, B. Cai, W. Feng, Y. Liu and H. Ma, Ceram. Int., 39, 8393–8400 (2013).
[15] B. Tchamba, U.C. Melo, G.L. Lecomte-Nana, E. Kamseu, C. Gault, R. Yongue and D. Njopwouo, Ceram. Int., 40, 1961–1970 (2014).
[16] E.Y. Sako, M.a.L. Braulio, A.P. Luz, E. Zinngrebe and V.C. Pandolfelli, J. Am. Ceram. Soc., 96, 3252–3257 (2013).
[17] M.A.L. Braulio, L.R.M. Bittencourt and V.C. Pandolfelli, Ceram. Forum Int., 85, 21–26 (2008).
[18] J.M. Auvray, C. Gault and M. Huger, J. Eur. Ceram. Soc., 27, 3489–3496 (2007).
[19] P. Nandi, A. Grag, B.D. Chattoraj and M.S. Mukhopadhyay, Am. Ceram. Soc. Bull., 31, 65–69 (2000).
[20] N.L. Hawari and M.R. Johan, J. Alloys Compd., 509, 2001–2006 (2011).
[21] R.a. Kleiv and M. Thornhill, Miner. Eng., 19, 340–347 (2006).
[22] J.P. Guha, Br. Ceram. Trans., 96, 231–236 (1997).
[23] R. Citak, J. Am. Ceram. Soc., 82, 237–240 (1999).
[24] V. Kumar, V.K. Singh, A. Srivastava and G.N. Agrawal, J. Am. Ceram. Soc., 95, 3769–3775 (2012).
[25] V. Kumar, V.K. Singh and A. Srivastava, J. Am. Ceram. Soc., 96, 2124–2131 (2013).
[26] P.C. Hewlett, Lea's Chemistry of Cement and Concrete, 4th ed., Arnold, London (2004), pp. 709–771.
[27] J.D. Birchall, A.J. Howard and K. Kendall, Nature, 289, 388–390 (1981).
[28] F. Ye, M. Rigaud, X. Liu and X.C. Zhong, Ceram. Int., 30, 801–805 (2004).
[29] S. Mukhopadhyay, S. Sen, T. Maiti, M. Mukherjee, R.N. Nandy and B.K. Sinhamahapatra, Ceram. Int., 29, 857–868 (2003).
[30] P.G. De La Iglesia, O. García-Moreno, R. Torrecillas and J.L. Menéndez, Ceram. Int., 38, 5325–5332 (2012).
[31] C. Domoanguez, J. Chevalier, R. Torrecillas, L. Gremillard and G. Fantozzi, J. Eur. Ceram. Soc., 21, 907–917 (2001).
[32] A. Srivastava, V.K. Singh, V. Kumar, P. Hemanth Kumar, H. Tripathi, A. Chaudhary, K. Asiwal, R. Pandey and S.K. Suman, J. Alloys Compd., 586, 581–587 (2014).
[33] P. Hemanth Kumar, A. Srivastava, V. Kumar, M.R. Majhi and V.K. Singh, J. Asian Ceram. Soc., 2, 169–175 (2014).
[34] A. Srivastava, V.K. Singh, V. Kumar and P. Hemanth Kumar, Ceram. Int., 40, 14061–14072 (2014).
[35] V. Kumar, V.K. Singh, A. Srivastava and P. Hemanth Kumar, Ceram. Int., 40, 16767–16777 (2014).
[36] N.M. Khalil, Br. Ceram. Trans., 103, 37–41 (2004).
[37] M.A. Serry, M.F. Zawrah and N.M. Khalil, Br. Ceram. Trans., 101, 165–168 (2002).
[38] M.F. Zawrah and N.M. Khalil, Ceram. Int., 27, 689–694 (2001).
[39] S.A. Abo-El-Enein, M.M. Abou-Sekkina, N.M. Khalil and O.A. Shalma, Ceram. Int., 37, 411–418 (2011).